IEEE Access
Multidisciplinary | Rapid Review | Open Access Journal

Received 19 July 2023, accepted 13 August 2023, date of publication 17 August 2023, date of current version 30 August 2023.

*Digital Object Identifier 10.1109/ACCESS.2023.3305950*

RESEARCH ARTICLE

# State-of-Charge Estimation Method for Lithium-Ion Batteries Using Extended Kalman Filter With Adaptive Battery Parameters

**JAEJUNG YUN[1], (Member, IEEE), YEONHO CHOI[1], JAEHYUNG LEE[1], SEONGGON CHOI[2], (Member, IEEE), AND CHANGSEOP SHIN[3], (Member, IEEE)**

[1]School of Electrical Engineering, Chungbuk National University, Cheongju 28644, South Korea
[2]School of Information and Communication Engineering, Chungbuk National University, Cheongju 28644, South Korea
[3]Department of Biosystems Engineering, Chungbuk National University, Cheongju 28644, South Korea

Corresponding author: Changseop Shin (shinchang7@chungbuk.ac.kr)

This work was supported by the Korean Institute of Planning and Evaluation for Technology in Food, Agriculture, Forestry (IPET) through Agriculture, and the Ministry of Agriculture, Food and Rural Affairs (MAFRA) (322043041440 31HD020), Korea Institute for Advancement of Technology (KIAT) grant funded by the Korea Government (MOTIE) (P0020536, HRD Program for Industrial Innovation), Basic Science Research Program through the National Research Foundation of Korea (NRF) funded by the Ministry of Education (No. 2020R1A6A1A12047945), and the MSIT (Ministry of Science and ICT), Korea, under the Grand Information Technology Research Center support program (IITP-2023-2020-0-01462) supervised by the IITP (Institute for Information & communications Technology Planning & Evaluation).

**ABSTRACT** Accurate battery state-of-charge (SOC) estimation is important for the efficient and reliable operation of battery application systems. The extended Kalman filter (EKF), which is based on the battery model, is widely used as a real-time SOC estimation algorithm; furthermore, its accuracy depends on the model accuracy. However, the conventional EKF uses one value for each battery parameter ($R_i$, $R_d$ and $C_d$) regardless of the SOC, even though their values change according to the SOC. To address this problem, this study proposes an improved EKF that applies battery parameters that change according to the SOC of a battery model. In the proposed method, the entire SOC was divided into several sections considering the deviation of the parameter values according to the SOC. Subsequently, the average values for each SOC section were calculated, and the values of the battery parameters were updated with the average values according to the SOC. To verify the performance of the proposed EKF, the parameters of commercial Li-ion batteries were extracted with dis-charge currents of 1C- and 2C-rates at ambient temperatures of 0 °C, 25 °C, and 45 °C, and MATLAB simulations were performed. Compared to the conventional EKF, the proposed EKF estimated the SOC more accurately under all the simulation conditions. Compared to the conventional EKF, the maximum reduced root-mean-square error and maximum error of the proposed method were 49.37% and 56.41%, respectively.

**INDEX TERMS** State of charge, lithium-ion battery, extended Kalman filter, battery parameter, battery model, battery management system.

## I. INTRODUCTION

Currently, lithium-ion batteries are the most widely used energy sources in eco-friendly industries. Energy storage devices for storing electric energy obtained through power generation such as solar, hydroelectric, and wind power, and battery packs used in electric vehicles require batteries with high energy density because it is efficient to store massive amounts of energy in the same volume. Lithium-ion batteries, lead-acid batteries, and nickel-cadmium batteries have energy densities of 500 Wh/L, 90 Wh/L, and 100 Wh/L, respectively [1]. Compared to the secondary batteries, lithium-ion batteries have a high energy density, low self-discharge, and high rated voltage; therefore, they are widely used in eco-friendly industries. However, improper charging and discharging can induce ignition and explosion in lithium-ion

The associate editor coordinating the review of this manuscript and approving it for publication was Enamul Haque.

batteries due to thermal runaway. Therefore, a battery management system is required to improve the performance of batteries and use them efficiently. A battery management system (BMS) has various functions to monitor the state of a battery and operate it in a stable region [2], [3], [4], [5]. The state of charge (SOC), one of the many important functions of a BMS, indicates the remaining capacity of the battery and is an important factor in determining its state. However, the SOC cannot directly indicate the internal state of a battery; therefore, it is usually indirectly estimated from the battery voltage, current, and temperature data [6], [7]. Representative SOC estimation methods include open-circuit voltage (OCV) measurements, Coulomb counting, extended Kalman filters (EKFs), and techniques that incorporate artificial intelligence algorithms [7], [8]. The OCV measurement method estimates the SOC based on the relationship in which the OCV of the battery matches the SOC in a ratio of 1:1. Although this method can be used to easily estimate the SOC, real-time estimation is impossible because a rest period is necessary for OCV voltage measurement. Coulomb counting estimates the SOC by integrating the current used when a battery is charged or discharged. It is widely used in industry because it enables real-time SOC estimation with a small amount of recall. However, it requires accurate information regarding the initial SOC value, and accumulates errors over time in the sensed current value. As deep learning technology has recently developed, the deep learning-based data-driven technique for estimating SOC using measurable battery data have been studied [9]. It does not require complicated battery model and electrochemical knowledge for SOC estimation by learning the relationship between battery data and SOC. As a result, a large amount of data is required for learning, but there is no need to model changes in battery parameters as well as nonlinear characteristics according to operating conditions or aging [10]. Recurrent Neural Network (RNN), one of these techniques, has a deep learning model structure that includes a loop in a hidden layer to maintain sequence information of the current time step. It can accurately map parameters such as voltage, current and temperature of the battery to the SOC. However, when using time-series data with long battery charge/discharge in the training phase, gradient vanishing is likely to occur. This makes it difficult to capture long-term dependencies of battery charge/discharge data, and thus degrades SOC estimation performance [11]. To solve this problem, deep learning models with gating mechanisms such as Long Short-Term Memory (LSTM) and Gated Recurrent Unit (GRU) were proposed. These enable more precise battery SOC estimation. In the case of the LSTM model, the long-term dependency problem is improved by determining valid memory information using an input gate, a forget gate, and an output gate. In addition, the GRU model improved the long-term dependency problem by using a reset gate and an update gate. This has the advantage of lower computational cost compared to LSTM models. As such, deep learning-based data-driven techniques are attracting much attention as future technologies for SOC estimation [12]. The EKF method estimates the SOC by calculating the OCV using a battery model. As it is robust against noise and enables real-time estimation, it is most widely used together with the Coulomb counting method. However, the battery model must accurately represent the electrochemical reactions of the battery and reflect the changes in the battery parameters according to the operating environment.

Representative battery models that are widely used include electrochemical model (EM) and electrical circuit model (ECM). The EM is constructed by interpreting the electrochemical action inside a battery cell. Although the accuracy of estimating the state of the battery is high, it is difficult to model. However, recently, high-performance electrochemical model-based algorithms based on ensemble Kalman filters have been proposed and many researches are being conducted [13], [14]. The ECM includes such electrical parameters as the resistance and capacitance extracted from the battery voltage and current waveforms during charging and discharging and can represent battery characteristics electrically. Although this model has lower accuracy than the EM, it is more widely used because of its easy implementation and applicability. In particular, the EKF usually uses a simple electrical model with a first- or second-order resistance–capacitance (RC) ladder, and the battery parameters are expressed as a single value regardless of the SOC section [15], [16], [17].

In the EKF, battery parameters are applied to the SOC estimation algorithm using the state-space equation. Therefore, the accuracy of the battery parameter values affects the battery SOC estimation [18]. Generally, each battery parameter in the EKF is defined as a single value; however, it changes according to the ambient temperature, C-rate, SOC, and charge/discharge cycles [19], [20], [21]. Therefore, the EKF, which uses a single parameter value without reflecting parameter changes in the battery, has an SOC estimation error. To address this problem, studies on EKF that reflect the changes in battery parameters have been conducted [6], [22], [23], [24]. In [6], a temperature compensation model, which incorporated temperature-dependent battery parameter changes into the Kalman filter, was added. The temperature compensation model expresses the diffusion resistance ($R_d$) and diffusion capacitance ($C_d$) as a quadratic expression of the SOC with coefficients that change according to the temperature and SOC using the data of the parameters in an offline experiment. Consequently, it is possible to estimate the SOC more accurately compared to that of the conventional method using a single value because the battery parameters can be updated according to the temperature and SOC. Other studies [22], [23] used dual EKFs and dual unscented Kalman filters to improve the accuracy of the battery model. Using dual filters, these methods reflect the battery parameters that change over time in real time in the battery model. In another study [24], the recursive least-squares algorithm was used to reflect battery parameters

dependent on the SOC in the model in real time. To improve the accuracy of the SOC estimation, the aforementioned methods [6], [22], [23], [24] increased the accuracy of the battery model; however, the battery model and estimation algorithm became complicated. As these methods require hardware such as expensive high-end computers or microprocessors to estimate the SOC of a battery, it is difficult to apply them to applications that use dozens to hundreds of cells (e.g., electric vehicles and energy storage systems).

Therefore, in this study, a method is proposed that has a higher SOC estimation accuracy than the conventional EKF, while also having a lower complexity than the existing improved EKF methods. The proposed method divides the SOC into several sections, and uses the representative values in each section to adapt the battery parameters $R_i$, $R_d$, and $C_d$ according to the SOC. As the parameter value of each battery differs based on the SOC, the deviation of these values was calculated. The SOC was divided into several sections using the calculated parameter deviations, and the average value of the parameters was calculated for each SOC section. the parameters were updated with average values and reflected in the battery model depending on the SOC section.

To verify the SOC estimation performance of the proposed EKF, battery parameters were extracted at various C-rates and outside temperatures, and MATLAB simulations were performed using these data. In the simulation, the SOC estimation accuracies and computation times of the conventional EKF, curve fitting-based EKF, forgetting factor recursive least squares(FRLS)-based EKF and proposed EKF were compared. In Section II, the relationship between the battery parameter values and accuracy of the SOC estimation is explained using the EKF and battery model. Section III provides the explanation on extraction of battery parameters and division of the SOC sections, and the adaptive battery parameters are defined. Section IV describes the proposed EKF, to which the adaptive battery parameters are applied. The SOC estimation accuracies and computation times of the proposed and previous EKFs were compared through simulations, as discussed in Section V, and the results were analyzed. Finally, Section VI summarizes the research content and describes the future research plans.

## II. BATTERY MODELING AND EXTENDED KALMAN FILTER

### A. BATTERY MODEL

A battery model is required to estimate the battery SOC using the EKF. In many cases, a first-order ECM is used, which can obtain a relatively high accuracy at a low computational cost [25]. A first-order ECM is composed of battery parameters, including the OCV ($V_{oc}$), internal resistance ($R_i$), diffusion resistance ($R_d$), and diffusion capacitance ($C_d$), which vary according to the temperature, C-rate, and SOC. In Fig. 1, $V_t$, $I_b$, $V_i$, and $V_{RC}$ represent the terminal voltage, battery current, voltage applied to the internal resistance, and RC ladder, respectively.

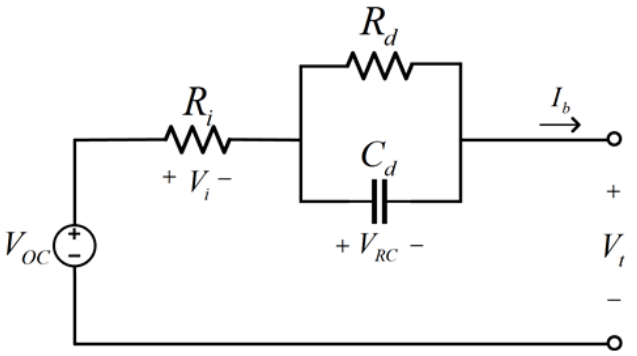


**FIGURE 1.** First-order ECM of battery.

### B. EXTENDED KALMAN FILTER FOR SOC ESTIMATION

#### 1) BATTERY STATE-SPACE EQUATIONS

EKF a recursive filter that estimates the state of a nonlinear system through measurements that contain noise. Its operation is as follows: state-vector prediction, Jacobian linearization, error-covariance prediction, Kalman gain calculation, calculation of the final estimate using the measured and predicted values, and error-covariance calculation [26]. Therefore, to estimate the SOC of a battery with nonlinear characteristics using the EKF, the following discrete state equations must be obtained:

In Fig. 1, $I_b$ is the sum of the currents flowing through $R_d$ and $C_d$, and can be expressed by the continuous state-space equation in (1).

$$I_b(t) = C_d \frac{dV_{RC}(t)}{dt} + \frac{V_{RC}(t)}{R_d} \tag{1}$$

By sampling (1) at time interval ($\Delta t$), the discrete state equation can be obtained as follows.

$$\frac{V_{RC}(k) - V_{RC}(k-1)}{\Delta t} = -\frac{V_{RC}(k-1)}{R_d C_d} + \frac{I_b(k-1)}{C_d} \tag{2}$$

By rearranging (2) into $V_{RC}(k)$, the following equation is obtained.

$$V_{RC}(k) = (1 - \frac{\Delta t}{R_d C_d})V_{RC}(k-1) + \frac{I_b(k-1)\Delta t}{C_d} \tag{3}$$

The SOC is defined as the ratio of the currently available battery capacity to the total capacity ($C_b$). It is expressed as (4) using the initial SOC ($SOC(0)$) and battery current ($I_b$) integrated during the battery charge/discharge time.

$$SOC(t) = SOC(0) - \int_0^t \frac{I_b(t)}{C_b} dt \tag{4}$$

The discrete state equation of the SOC is given by sampling (4) as follows.

$$SOC(k) = SOC(k-1) - \frac{I_b(k-1)\Delta t}{C_b} \tag{5}$$

From (3) and (5), the state equation matrix applied to the EKF is as follows:

$$\begin{bmatrix} SOC(k) \\ V_{RC}(k) \end{bmatrix} = \begin{bmatrix} 1 & 0 \\ 0 & 1-\frac{\Delta t}{R_d C_d} \end{bmatrix} \begin{bmatrix} SOC(k-1) \\ V_{RC}(k-1) \end{bmatrix} + \begin{bmatrix} -\frac{\Delta t}{C_b} \\ \frac{\Delta t}{C_d} \end{bmatrix} I_b(k-1) \quad (6)$$

The terminal voltage $V_t$ is represented by

$$V_t = V_{OC} - V_{RC} - R_i I_b \quad (7)$$

By linearizing (7) through the Jacobian and sampling it, the following discrete output equation for $V_t$ can be obtained.

$$V_t(k) = \begin{bmatrix} \frac{\partial OCV}{\partial SOC}\big|_{SOC} & -1 \end{bmatrix} \begin{bmatrix} SOC(k-1) \\ V_{RC}(k-1) \end{bmatrix} - R_i I_b(k-1) \quad (8)$$

The discrete state-space equation of the system commonly used in the EKF is as follows.

$$\begin{cases} x_k = Ax_{k-1} + Bu_{k-1} + w_{k-1} \\ y_k = Hx_k + Du_k + v_k \end{cases} \quad (9)$$

where $x_k$, $u_k$, $y_k$, $w_k$, and $w_k$ are the state variable, input variable, output variable, process noise, and measured noise, respectively.

To estimate the battery SOC, matrices $A$, $B$, $H$, and $D$ in the discrete state-equation of (9) are defined by (6) and (8).

The matrices are

$$A = \begin{bmatrix} 1 & 0 \\ 0 & 1-\frac{\Delta t}{R_d C_d} \end{bmatrix}, \; B = \begin{bmatrix} -\frac{\Delta t}{C_b} \\ \frac{\Delta t}{C_d} \end{bmatrix}$$
$$H = \begin{bmatrix} \frac{\partial OCV}{\partial SOC}\big|_{SOC} & -1 \end{bmatrix}, \; D = R_i \quad (10)$$

#### 2) PROCESS OF ESTIMATING SOC USING THE EKF

Fig. 2 shows the battery SOC estimation process using the EKF. The EKF used in this model predicted and estimated the state vector and error covariance using the battery parameters ($R_i$, $R_d$, and $C_d$) of the first-order ECM of the battery. The estimated value of the state vector ($[SOC(k)\ V_{RC}(k)]^T$) consists of its predicted value of the state vector ($[SOC^-(k)\ V_{RC}^-(k)]^T$) and the prediction error of the measured value ($V_t(k) - \hat{V}_t(k)$), which is used to correct the predicted value. Therefore, the process of calculation and correction of the accurately predicted values significantly affects the estimation accuracy of the EKF.

The prediction process of the SOC estimation using the EKF can be expressed by (11) and (12) to calculate the predicted value of the state vector and of the error covariance, respectively.

$$\begin{bmatrix} SOC^-(k) \\ V_{RC}^-(k) \end{bmatrix} = \begin{bmatrix} 1 & 0 \\ 0 & 1-\frac{\Delta t}{R_d C_d} \end{bmatrix} \begin{bmatrix} SOC(k-1) \\ V_{RC}(k-1) \end{bmatrix} + \begin{bmatrix} -\frac{\Delta t}{C_b} \\ \frac{\Delta t}{C_d} \end{bmatrix} I_b(k-1) \quad (11)$$

$$P^-(k) = \begin{bmatrix} 1 & 0 \\ 0 & 1-\frac{\Delta t}{R_d C_d} \end{bmatrix} P(k-1) \times \begin{bmatrix} 1 & 0 \\ 0 & 1-\frac{\Delta t}{R_d C_d} \end{bmatrix}^T + Q \quad (12)$$

Equations (11) and (12) provide the accurate mean and variance of the predicted value of the state vector, respectively. The equations were calculated using the battery parameters, and the application of accurate battery parameters increased the estimation accuracy of the EKF. (8) represents the predicted value of the battery terminal voltage, and is used to estimate the SOC by correcting the predicted value, as in (13).

$$\begin{bmatrix} SOC(k) \\ V_{RC}(k) \end{bmatrix} = \begin{bmatrix} SOC^-(k) \\ V_{RC}^-(k) \end{bmatrix} + K(k)(V_t(k) - \hat{V}_t(k)) \quad (13)$$

where K is the Kalman gain and is used as a weight for the predicted value correction. To accurately calculate the prediction error of the measured value, an accurate measured value of the terminal voltage ($V_t$) and the predicted value of the terminal voltage ($\hat{V}_t$) are required. The terminal voltage can be accurately measured using a sensor with a low error. Thus, the prediction error of the accurate measurement value was determined by accurately calculating the terminal voltage. The terminal voltage is expressed as (14).

$$\hat{V}_t(k) = V_{OC}(k) - \left(1 - \frac{\Delta t}{R_d C_{d\,i}}\right) V_{RC}(k) - \left(\frac{\Delta t}{C_d} + R_i\right) I_b(k) \quad (14)$$

The terminal voltage was calculated using the battery parameters. The battery parameters varied depending on the SOC. Therefore, to accurately estimate the SOC using the EKF, changes in the battery parameters had to be applied. The estimated values were affected by the predicted value and prediction error of the measured value, and these values were calculated based on the battery parameters. Therefore, to improve the estimation accuracy of the EKF, it is necessary to apply battery parameters that vary according to the SOC, rather than single parameters.

## III. ADAPTIVE BATTERY PARAMETERS

### A. BATTERY PARAMETER EXTRACTION

The battery parameters $R_i$, $R_d$, and $C_d$ of the first-order ECM shown in Fig. 1 can be extracted through a pulse-current discharge experiment (Fig. 3(a)). The pulse-discharge experiment was performed by repeating the discharging and rest operations at a constant SOC interval ($I$) from the charging cutoff voltage to the discharging cutoff voltage. For battery parameter extraction, the total number ($N_p$) of SOC points is determined by the designated SOC interval ($I$) at the discharge and rest operations. $N_p$ is 100 divided by $I$, and the battery parameters according to the SOC are defined as discrete values at each SOC point. The pulsed-current discharge experiment cannot obtain continuous parameters according to the SOC; however, the experiment is simple and widely used as a battery parameter extraction technique. In this study,

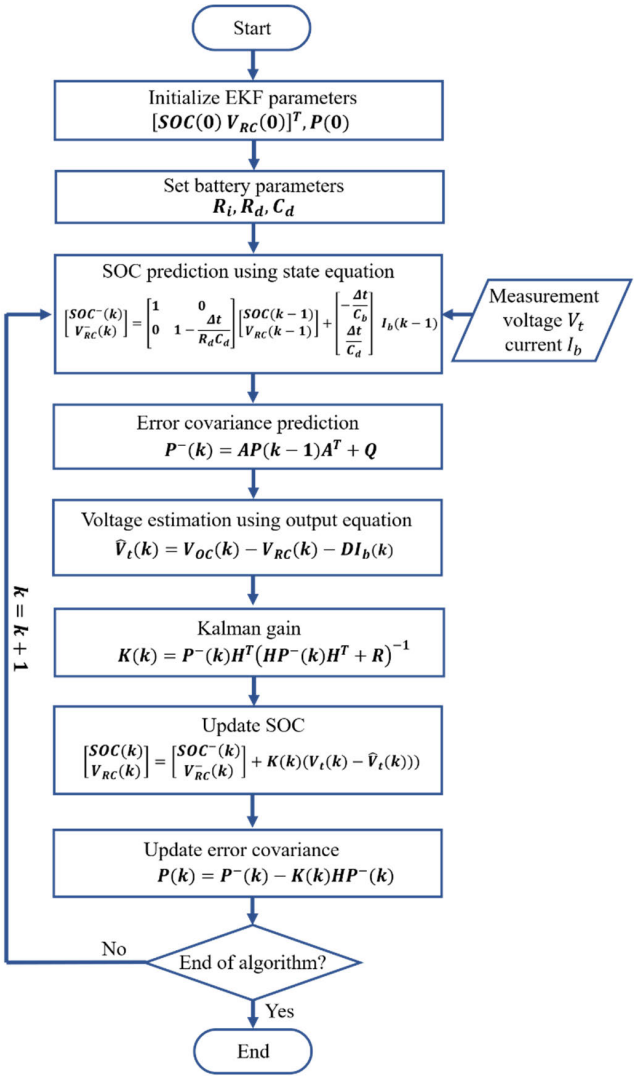


**FIGURE 2.** Flowchart of SOC estimation algorithm using the conventional EKF.

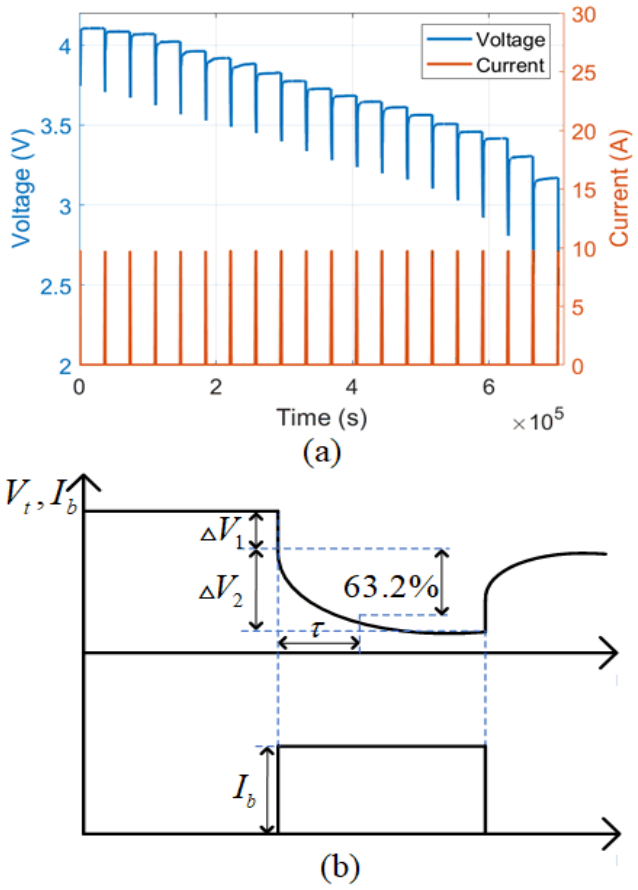


**FIGURE 3.** Battery pulse-current discharging experiment for extracting battery parameters: (a) pulse-current discharge in 5% increments of SOC and (b) battery terminal voltage ($V_t$) response curve at single current discharge pulse ($I_b$).

**TABLE 1.** Main specifications of INR21700-50E.

| Parameter | Value |
|---|---|
| Nominal capacity | 4900 mAh |
| Charging cutoff voltage | 4.2 V |
| Nominal voltage | 3.7 V |
| Discharging cutoff voltage | 2.5 V |

experiments were conducted at 5% SOC intervals, considering the tradeoff relationship between the accuracy of the parameters and the amount of computation required for SOC estimation.

The battery voltage and current waveforms for a single-pulse discharge are shown in Fig. 3(b). Here, $\Delta v_1$ is the voltage drop of the battery at the moment when the battery starts discharging, $\Delta v_2$ is the voltage drop that gradually decreases owing to the battery discharge current $I_b$, and $\tau$ is the time it takes for the battery to start discharging and decrease the voltage to 63.2% of $\Delta v_2$. When a single-discharge pulse waveform was applied to the battery, the first-order ECM exhibited five operating modes. Equations (15)–(17) for extracting the battery parameters can be derived from the analysis of each operation mode [6], [27].

When the discharge pulse current is applied, it can be approximated that the $C_d$ of the ECM is shorted owing to high-frequency operation. Therefore, $\Delta v_1$ represents the voltage drop of $R_i$.

$$R_i = \frac{\Delta v_1}{I_b} \tag{15}$$

Here, $\Delta v_2$ is the battery voltage drop caused by the first RC ladder of the ECM, and $R_d$ and $C_d$ can be obtained from (16) and (17).

$$R_d = \frac{\Delta v_2}{I_b} \tag{16}$$

$$C_d = \frac{\tau}{R_d} \tag{17}$$

The commercial battery model for the experiment was a Samsung INR 21700-50E, and its main specifications are listed in Table 1.

To extract the battery parameters ($R_i$, $R_d$, and $C_d$), pulse-current discharge experiments were performed at 5% inter-

vals of the SOC with currents of 1C- and 2C-rates at ambient temperatures of 0, 25, and 45 °C. Fig. 4 shows the battery parameters obtained from the experiment. The battery model parameters were changed according to the SOC at different C-rates and temperatures.

### B. PROPOSED SOC SECTION AND ADAPTIVE BATTERY PARAMETER

As shown in Fig. 4, the battery parameters ($R_i$, $R_d$, and $C_d$) changed according to the SOC. Therefore, when each battery parameter was defined as a single value, deviations occurred between the defined and actual values depending on the SOC. The deviation in the battery parameters according to the SOC caused an SOC estimation error when the EKF was used, as described in section B of part II. To address this problem, a method was developed to apply battery parameters adapted according to the SOC to the EKF. As in an earlier report [6], the adaptive battery parameters can be expressed as functions according to the SOC. However, this method has a disadvantage in that the number of computations increases significantly. It is difficult to apply this method to commercial SOC algorithms using the EKF for battery applications. Therefore, in the proposed method, battery parameters are defined as constants adapted according to the SOC. To obtain the adaptive battery parameters, the entire SOC was divided into several sections considering the deviation of the battery parameter values according to the SOC. Subsequently, the average values of the battery parameters for the SOC sections were calculated, and the adaptive battery parameters were updated with the average values according to the SOC. The adaptive battery parameters $R_i$, $R_d$, and $C_d$ were individually defined using the aforementioned methods.

The SOC estimation accuracy can be expressed by SOC estimation errors, such as the maximum error and root mean square error (RMSE). The maximum error and RMSE for the SOC estimation depend on the maximum deviation rate ($DV_{max}$) and standard deviation ($SD$) between the average and actual values of the battery parameters, respectively. For the proposed EKF to have a higher SOC estimation accuracy than the conventional EKF, $DV_{max}$ and $SD$ of the proposed method using SOC section segmentation must be smaller than those of the conventional method, which uses one value for each parameter. To satisfy these conditions, SOC section segmentation must be performed according to the seven procedures given in (Fig. 5).

(1) Set the initial value of number($N$) of SOC sections

In order to start the SOC division of the proposed method, an initial value of $N$ must set. The proposed method divides the entire SOC into $N$ sections and applies the average value of each section to the EKF. Therefore, the initial value of $N$ is selected as 2, which is the minimum value of the section division.

(2) Division of the entire SOC into N SOC sections

After $N$ is set, the entire SOC is divided into $N$ SOC sections as follows: First, the deviation $\Delta P[m]$ between the parameter values at two adjacent SOC points was calculated as follows:

$$\Delta P[m] = |P[m+1] - P[m]| \tag{18}$$

where $P[m]$ and $P[m+1]$ denote the battery parameter values at the $m$th and $(m+1)$th SOC points, respectively, for the entire SOC.

Next, $(N_p - 1)$ $\Delta P$s (= $\Delta P$ [1], $\Delta P$ [2], $\cdots \Delta P[N_p - 1]$) was calculated using (18). Here, $N_p$ is the total number of SOC points. To divide the SOC into $N$ SOC sections, $(N-1)$ SOC points for the section boundaries were required, and these were obtained from $(N-1)$ $\Delta P$s. At this time, $(N-1)$ $\Delta P$s were selected in the order of the greatest value among the $(N_p-1)$ $\Delta P$s. This is because the $DV_{max}$ and SD of the battery parameters were reduced further when the SOC sections were divided based on a larger $\Delta P$. Among the two adjacent SOC points for the selected $\Delta P$, one point that could more effectively improve the deviation of the parameters was used as a boundary point. Then, $(N-1)$ boundary points were selected for $(N-1)$ $\Delta P$s in the same manner.

(3) Calculation of $DV_{max,pro}$, and $SD_{pro}$

To improve the SOC estimation accuracy, the maximum deviation rate ($DV_{max,pro}$) and standard deviation ($SD_{pro}$) of the proposed method should be smaller than the maximum deviation rate ($DV_{max,con}$) and standard deviation ($SD_{con}$) of the conventional method. To achieve this, it is first necessary to calculate the $DV_{max,pro}$ and $SD_{pro}$ of the proposed method.

Here, $P_{avg}[K]$ is the average of the battery parameter values in the $K$th SOC section

$$P_{avg}[K] = \sum_{m=1}^{n_k} P[K_m] \Big/ n_k \tag{19}$$

where $P[K_m]$ and $n_K$ are the battery parameter values at the $m$th SOC point and the total number of SOC points in the $K$th SOC section, respectively.

Each SOC section includes the battery parameter values at the section boundaries.

$DV[K_m]$ at the $K_m$th SOC point is the deviation between the real value of the battery parameters at the corresponding SOC point and average value of the battery parameters in the $K$th SOC section, and it is calculated using the following equation:

$$DV[K_m] = \frac{|P[K_m] - P_{avg}[K]|}{P_{avg}[K]} \times 100 \tag{20}$$

Among all the $DV$s of the proposed method, $DV_{max,pro}$ had the largest deviation rate.

As the battery parameter values at the section boundaries are used in duplicate, the total number of parameter values becomes $(N_p + N - 1)$ to calculate the $SD_{pro}$. The $SD_{pro}$ is

$$SD_{pro} = \sqrt{\sum_{K=1}^{N} \sum_{m=1}^{n_K} (P[K_m] - P_{avg}[K])^2 \Big/ N_p + N - 1} \tag{21}$$

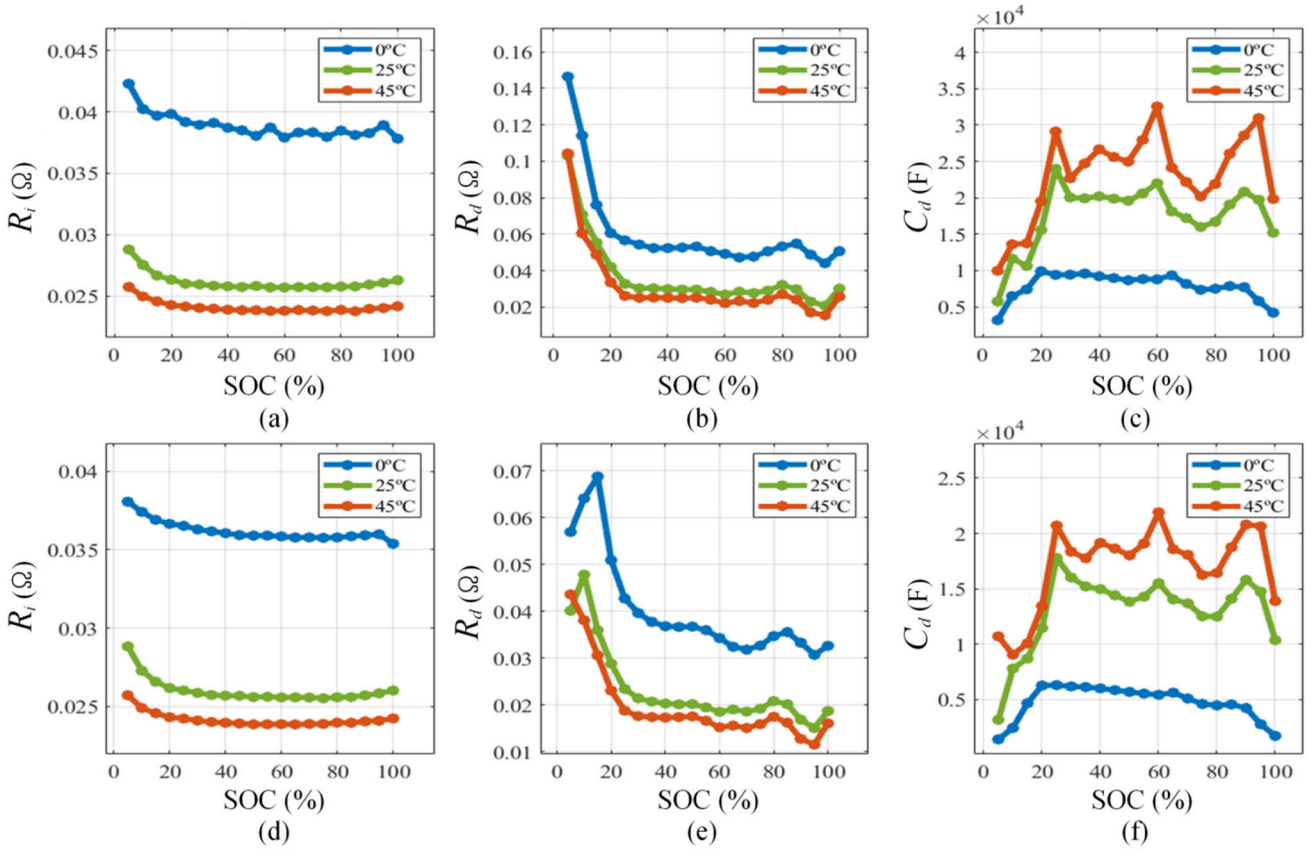


**FIGURE 4.** Battery parameters according to SOC at different C-rates and temperatures: (a) $R_i$ at 1C-rate, (b) $R_d$ at 1C-rate, (c) $C_d$ at 1C-rate, (d) $R_i$ at 2C-rate, (e) $R_d$ at 2C-rate, and (f) $C_d$ at 2C-rate.

(4) Comparison of parameter deviation between the conventional method and the proposed method

For the proposed EKF to have a higher SOC estimation accuracy than the conventional EKF, $DV_{max}$ and $SD$ of the proposed method using SOC section segmentation must be smaller than those of the conventional method, which uses one value for each parameter. To compare the deviation between the conventional method and proposed method, the $DV_{max,con}$ and $SD_{con}$ should be calculated through (22)-(24).

The average value ($P_{avg}$) of the battery parameter in the conventional method is the average of $N_p$ battery parameter values and is given by

$$P_{avg} = \sum_{n=1}^{N_p} P[n] \Big/ N_p \tag{22}$$

where $P[n]$ is the battery parameter value at the $n_{th}$ SOC point in the entire SOC range, and $N_p$ is the total number of SOC points. The average values of $R_i$, $R_d$, and $C_d$ were individually calculated using (22).

$DV_{max,con}$ and $SD_{con}$ are given by

$$DV_{\max,con} = \frac{|P[n] - P_{avg}|}{P_{avg}} \times 100 \tag{23}$$

$$SD_{con} = \sqrt{\sum_{n=1}^{N_p} (P[n] - P_{avg})^2 \Big/ N_p} \tag{24}$$

The calculated $DV_{max,pro}$, $SD_{pro}$, $DV_{max,con}$, and $SD_{con}$ are compared using conditional expression (25).

$$DV_{max,pro} < DV_{max,con} \text{ and} SD_{pro} < SD_{con} \tag{25}$$

If the $DV_{max,pro}$ and $SD_{pro}$ of the proposed method are greater than the $DV_{max,con}$ and $SD_{con}$ of the conventional method, increase $N$ by 1 and return to step 2. Otherwise, go to step 5.

(5) SOC estimation using EKF

If the condition in step 4 is satisfied, the average values of the battery parameters ($R_i$, $R_d$, and $C_d$) in the divided sections according to SOC are applied to the battery model. Then, the SOC is estimated by EKF with this battery model.

(6) Comparison of calculated and target SOCs

Compare whether the SOC calculated through step 5 satisfies the target SOC required by the user or application. Target SOC is determined within the range of optimal $N$ shown in Fig. 6 by considering the tradeoff between the SOC estimation accuracy and the amount of computation.

If the calculated SOC dose not satisfy the target SOC, increase $N$ by 1 and return to step 2. Otherwise, go to step 7.

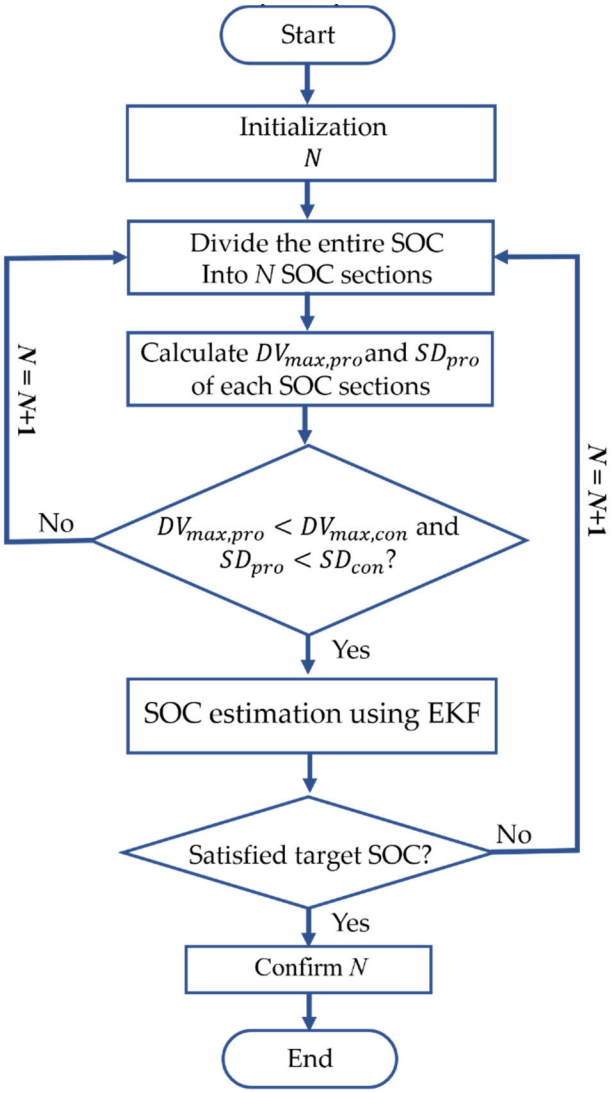


**FIGURE 5.** Flowchart of verification of the number of SOC sections in the proposed method.

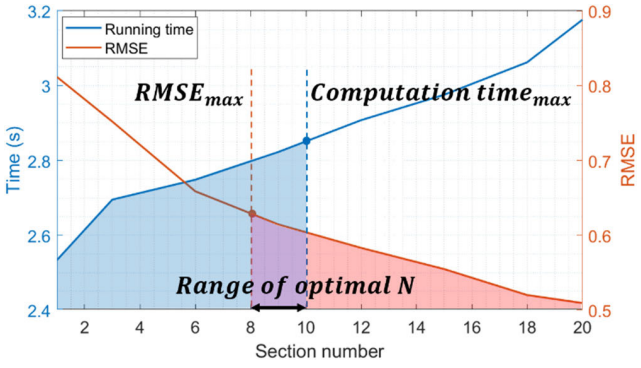


**FIGURE 6.** RMSE and computation time according to the section number.

(7) The number of sections is determined as the current value of $N$

The optimal $N$ is determined through steps 1 to 6.

In this paper, the proposed method aimed to have a higher SOC estimation accuracy than the conventional EKF, and to satisfy this, $N$ was determined as 3 by the flowchart in Fig. 5. Figs. 7 and 8 show the battery parameters ($R_i$, $R_d$, and $C_d$) in Fig. 4 divided into three SOC sections using the proposed method. To divide the SOC into three SOC sections, two SOC points for the section boundaries were obtained from the first and second largest $\Delta P$s. Among the two adjacent SOC points for the selected $\Delta P$, the SOC point on the left was used as the section boundary. $DV_{max,con}$, $SD_{con}$, $DV_{max,pro}$, and $SD_{pro}$ values were calculated by substituting the values of $R_i$, $R_d$, and $C_d$ in Fig. 4 into (19)-(21) and (22)-(24), are listed in Tables 2 and 3, respectively. Table 4 shows the percentage decrease in $DV_{max}$ and $SD$ of the battery parameters owing to the proposed method. This satisfies conditional expression (25). When the optimal $N$ is determined to be 3, the SOC estimation performances of EKFs are given to the simulation results of Section V.

## IV. PROPOSED EXTENDED KALMAN FILTER WITH ADAPTIVE BATTERY PARAMETERS

In a conventional EKF, each battery parameter is defined as a single value regardless of the SOC. Consequently, the SOC estimation accuracy is reduced. In contrast, the proposed EKF divides the SOC sections and updates the adaptive battery parameters according to the SOC. This update process makes the values of the battery parameters more accurate, which increases the accuracy of the predicted and estimated values of the state variables SOC and $V_{RC}$ in the EKF algorithm. Therefore, the proposed EKF has a high SOC estimation accuracy. Fig. 9 shows the SOC estimation process using the proposed EKF.

## V. SIMULATION

MATLAB simulations were performed to verify the performance of the proposed EKF with adaptive battery parameters. For each battery parameter, the proposed method was compared with the conventional EKF using a single value. The SOC estimation accuracies of the two methods were calculated using the SOC estimated from the Coulomb counting method as the reference value. The data for the battery parameters shown in Figs. 4, 7, and 8 are used in the simulation. The $DV_{max}$ and $SD$ of each battery parameter according to the SOC in the proposed method and conventional EKF were calculated from these data, as shown in Tables 2 and 3. The $DV$ and $SD$ values in the proposed method were lower than those in the conventional EKF under all ambient temperatures and C-rate test conditions (see Table 4).

Fig. 10 shows the SOC estimation results of the proposed method and conventional EKF when the battery is discharged with a 1C-rate pulse current at three ambient temperatures (0, 25, and 45 °C). At an ambient temperature of 0 °C, the RMSE for SOC estimation in the conventional EKF was 1.3578, and that in the proposed EKF was 1.2572, thus reducing the error by 7.41%. Additionally, the conventional

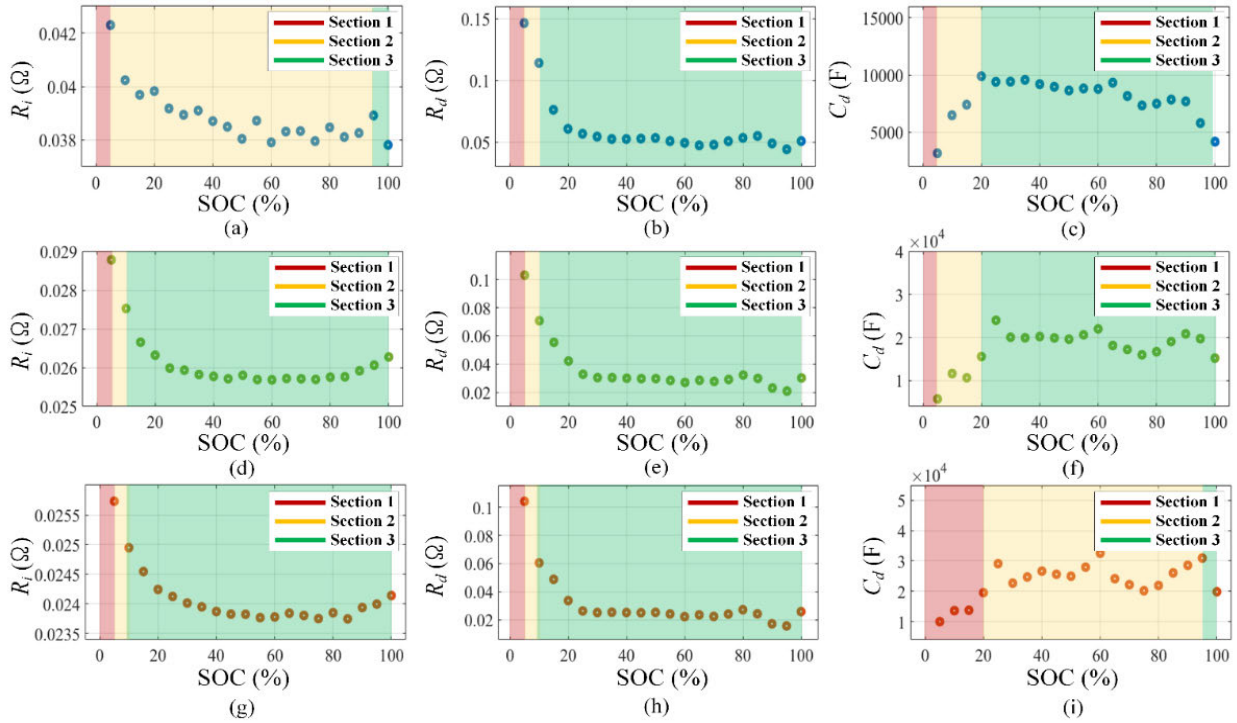


**FIGURE 7.** Battery parameter curves divided into three SOC sections by the proposed method at 1C-rate: (a) $R_i$ at 0 °C, (b) $R_d$ at 0 °C, (c) $C_d$ at 0 °C, (d) $R_i$ at 25 °C, (e) $R_d$ at 25 °C, (f) $C_d$ at 25 °C, (g) $R_i$ at 45 °C, (h) $R_d$ at 45 °C, and (i) $C_d$ at 45 °C.

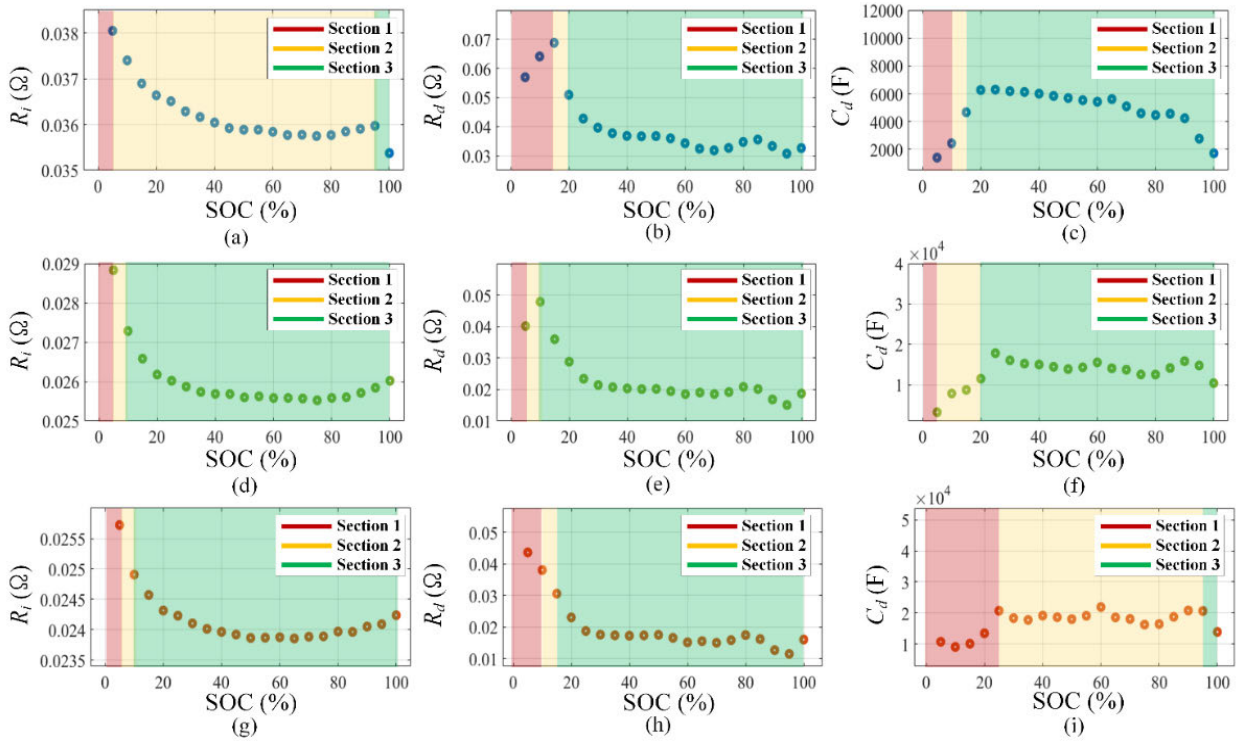


**FIGURE 8.** Battery parameter curves divided into three SOC sections by the proposed method at 2C-rate: (a) $R_i$ at 0 °C, (b) $R_d$ at 0 °C, (c) $C_d$ at 0 °C, (d) $R_i$ at 25 °C, (e) $R_d$ at 25 °C, (f) $C_d$ at 25 °C, (g) $R_i$ at 45 °C, (h) $R_d$ at 45 °C, and (i) $C_d$ at 45 °C.

EKF has a maximum SOC estimation error of 5.3596% at the SOC 5% point, whereas the proposed EKF has a maximum error of 5.311% at the SOC 5% point, thus reducing the error by approximately 0.91%, as shown in Figs. 10(a) and (d). Figs. 10(b) and (e) show the SOC estimation results of the two methods at an ambient temperature of 25 °C. As shown in

**TABLE 2.** Comparison of $DV_{max}$ and $SD$ of battery parameters between the conventional EKF and proposed EKF at 1C-rate.

| | | Conventional Method | | Proposed Method | |
|---|---|---|---|---|---|
| $T$ | Parameter | $DV_{max}$ (%) | $SD$ | $DV_{max}$ (%) | $SD$ |
| 0°C | $R_i$ | 8.83 | 0.001019 | 3.88 | 0.000623 |
| | $R_d$ | 140.63 | 0.024500 | 43.25 | 0.007520 |
| | $C_d$ | 59.79 | 1758.63 | 49.44 | 1269.591 |
| 25°C | $R_i$ | 10.14 | 0.000745 | 2.90 | 0.000282 |
| | $R_d$ | 181.67 | 0.018828 | 78.91 | 0.007631 |
| | $C_d$ | 67.46 | 4195.4016 | 24.17 | 2123.830 |
| 45°C | $R_i$ | 6.82 | 0.000475 | 2.50 | 0.000206 |
| | $R_d$ | 233.66 | 0.019400 | 38.93 | 0.006358 |
| | $C_d$ | 57.15 | 5747.57 | 37.49 | 3377.142 |

**TABLE 3.** Comparison of $DV_{max}$ and $SD$ of battery parameters between the conventional EKF and proposed EKF at 2C-rate.

| | | Conventional Method | | Proposed Method | |
|---|---|---|---|---|---|
| $T$ | Parameter | $DV_{max}$ (%) | $SD$ | $DV_{max}$ (%) | $SD$ |
| 0 °C | $R_i$ | 5.16 | 0.000620 | 3.53 | 0.000418 |
| | $R_d$ | 70.93 | 0.107700 | 19.22 | 0.003768 |
| | $C_d$ | 70.40 | 1488.26 | 66.22 | 1120.798 |
| 25 °C | $R_i$ | 10.85 | 0.000760 | 3.11 | 0.000299 |
| | $R_d$ | 105.65 | 0.008723 | 71.56 | 0.004388 |
| | $C_d$ | 75.73 | 3293.41 | 27.79 | 1618.541 |
| 45 °C | $R_i$ | 6.43 | 0.000440 | 2.22 | 0.000195 |
| | $R_d$ | 93.33 | 0.008042 | 39.39 | 0.002501 |
| | $C_d$ | 46.85 | 3614.81 | 24.27 | 1621.482 |

**TABLE 4.** Percentage decrease in $DV_{max}$ and $SD$ of battery parameters for the proposed method.

| | | 1C-rate | | 2C-rate | |
|---|---|---|---|---|---|
| $T$ | Parameter | $P_{DVmax}$ (%) | $P_{SD}$ (%) | $P_{DVmax}$ (%) | $P_{SD}$ (%) |
| 0 °C | $R_i$ | 56.08 | 38.85 | 31.59 | 32.51 |
| | $R_d$ | 69.25 | 69.30 | 72.90 | 96.50 |
| | $C_d$ | 17.31 | 27.80 | 5.94 | 24.69 |
| 25 °C | $R_i$ | 71.44 | 62.13 | 71.34 | 60.55 |
| | $R_d$ | 56.57 | 59.46 | 32.27 | 49.69 |
| | $C_d$ | 64.17 | 49.37 | 63.30 | 50.85 |
| 45 °C | $R_i$ | 63.34 | 56.58 | 65.47 | 55.53 |
| | $R_d$ | 83.34 | 67.22 | 57.81 | 68.89 |
| | $C_d$ | 34.40 | 41.24 | 48.20 | 55.15 |

Table 2, as the $DV$ and $SD$ of the battery parameters reduced, the RMSE and maximum error of the SOC estimation in the proposed EKF decreased compared with those in the conventional EKF. The RMSE and maximum error of the SOC estimation in the proposed EKF were 0.752 and 2.8338% (at the SOC 3% point), respectively. As in the previous two simulation results, the proposed EKF improved the accuracy of SOC estimation by updating the battery parameters according to the SOC, even under an ambient temperature condition of 45 °C. The RMSE for SOC estimation in the conventional EKF was 0.6884, and that in the proposed EKF was 0.4774, reducing the error by 30.65%. Furthermore, the conventional EKF had a maximum SOC estimation error of 3.8198% at the SOC 5% point, whereas the proposed EKF had a maximum error of 2.4351% at the SOC 10% point, thus reducing the error by approximately 36.25%.

**TABLE 5.** Comparison of SOC estimation errors between the proposed and conventional EKFs.

| C-rate | $T$ | RMSE | | | Maximum Error | | |
|---|---|---|---|---|---|---|---|
| | | Basic EKF | Proposed EKF | $R_{RMSE}$ | Basic EKF | Proposed EKF | $R_{MAX}$ |
| 1C-rate | 0 °C | 1.3578 | 1.2572 | 7.41% | 5.3596% | 5.311% | 0.91% |
| | 25 °C | 0.8116 | 0.752 | 7.34% | 3.302% | 2.8338% | 14.18% |
| | 45 °C | 0.6884 | 0.4774 | 30.65% | 3.8198% | 2.4351% | 36.25% |
| 2C-rate | 0 °C | 1.6038 | 0.8865 | 44.73% | 4.9659% | 2.1646% | 56.41% |
| | 25 °C | 1.9947 | 1.3605 | 31.79% | 4.5096% | 3.7049% | 8.74% |
| | 45 °C | 0.9067 | 0.4591 | 49.37% | 4.1887% | 1.828% | 56.36% |

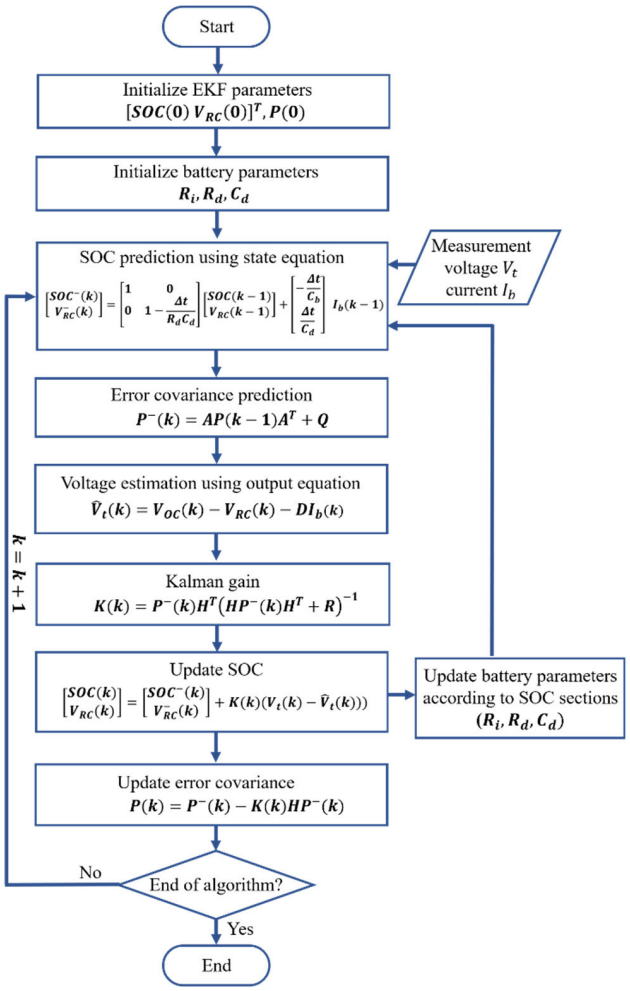


**FIGURE 9.** Flowchart of SOC estimation algorithm using the proposed EKF.

Fig. 11 shows the SOC estimation results of the proposed method and conventional EKF when the battery is discharged with a 2C-rate pulse current at ambient temperatures of 0, 25, and 45 °C. Under the above test conditions, the proposed EKF reduced the *DV* and *SD* of the parameters compared with the conventional EKF by updating the battery parameters to an average value for each SOC section (Table 3). This is similar to the simulation results at a 1C-rate, the proposed EKF improved the RMSE and maximum error of the SOC estimation under all the simulation conditions. The results are listed in Table 5. $R_{RMSE}$ and $R_{MAX}$ represent the decrease in percentage in the RMSE and maximum error for the proposed EKF, respectively. Compared to the conventional EKF, the maximum reduced RMSE and maximum error for the proposed method were 49.37% (at 2C-rate and 45 °C) and 56.41% (at 2C-rate and 0 °C), respectively. The simulation results verify that the proposed method using adaptive battery parameters can improve the SOC estimation accuracy of the EKF.

To analyze the estimated performance according to section number, simulation was conducted on an AMD Ryzen 7 PRO 4750G, 3.60GHz CPU and 16GB RAM PC. The SOC estimation results and the estimated performance of each EKF with section numbers 1, 3, and 20 are shown in Fig. 12 and Table 6, respectively.

The RMSE and maximum SOC estimation error of the EKF with 20 sections are 0.5094 and 2.3504%, respectively. The computation time was 3.1761 s. As the number of SOC sections increased, the values of the battery parameters approached the real values at each SOC, thus resulting in the increase of SOC estimation accuracy. However, as the number of SOC sections increased, the amount of computation also increased, resulting in a longer computation time.

To validate the superiority of the proposed method, it was compared the improved EKFs in [28] and [29], which use adaptive battery parameters. For comparison, a battery data set from the Center for Advanced Life Cycle Engineering (CALCE) at the University of Maryland was used, which consists of pulse discharge data and Dynamic Stress Test (DST) [30]. The model of the battery is INR 18650-20R and its specifications are given in Table 7.

The battery parameters ($R_i$, $R_d$ and $C_d$) extracted from the pulse discharge data are given in Fig. 13, and each parameter is divided into three sections using the proposed method (Fig. 14). The extracted battery parameters were used for the conventional EKF, the curve fitting-based EKF of [28] and the proposed EKF. The forgetting factor recursive least squares (FRLS) method of [29] estimated the battery parameters using the voltage and current of DST. Then, the SOC RMSE and computation time of these EKFs were compared

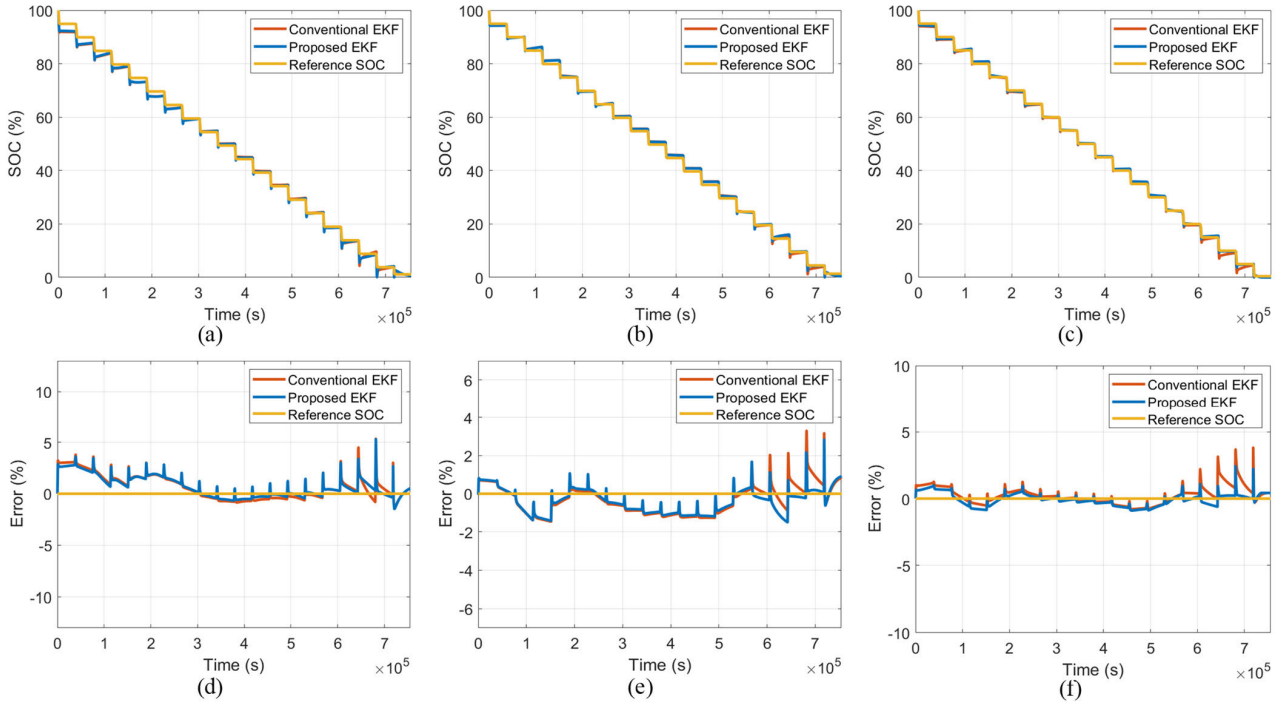


**FIGURE 10.** Simulation results at 1C-rate: (a) SOC estimation at 0 °C, (b) SOC estimation at 25 °C, (c) SOC estimation at 45 °C, (d) SOC estimation error at 0 °C, (e) SOC estimation error at 25 °C, and (f) SOC estimation error at 45 °C.

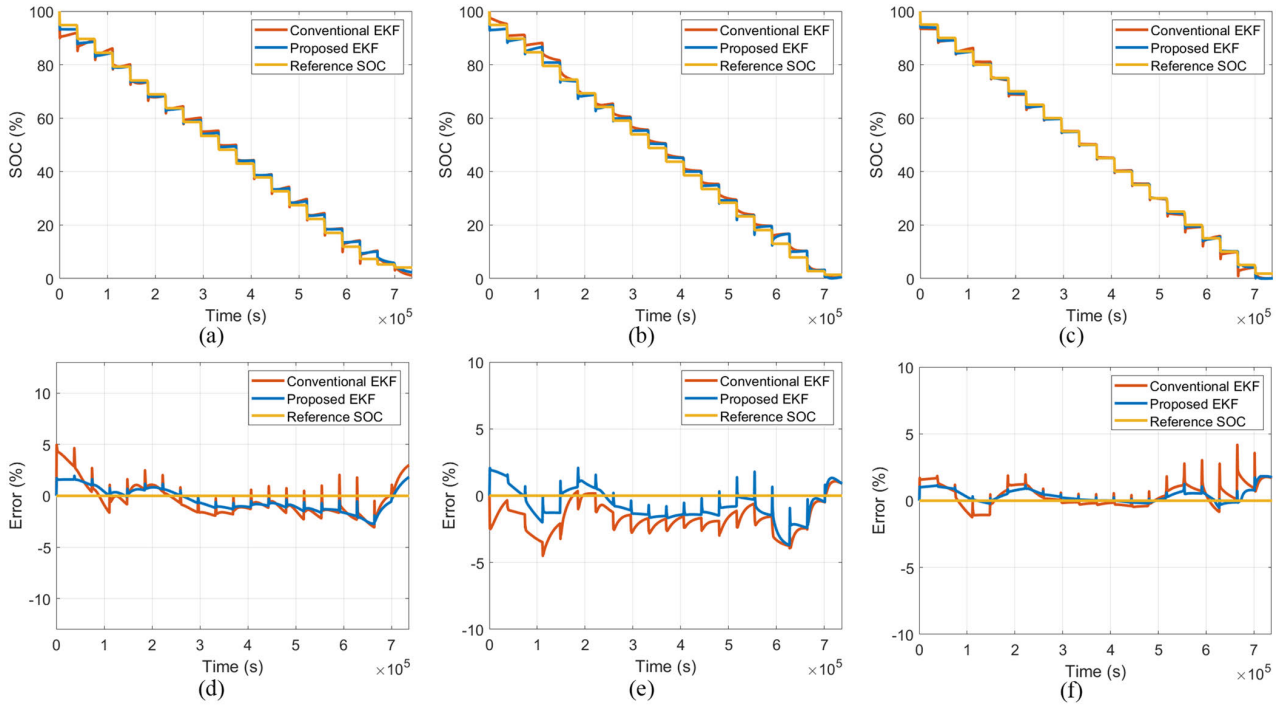


**FIGURE 11.** Simulation results at 2C-rate: (a) SOC estimation at 0 °C, (b) SOC estimation at 25 °C, (c) SOC estimation at 45 °C, (d) SOC estimation error at 0 °C, (e) SOC estimation error at 25 °C, and (f) SOC estimation error at 45 °C.

using the DST data (Figs. 15 and 16). Here, the curve fitting method fitted a battery parameter with the 6th polynomial using MATLAB's cftool and the FRLS method selected a forgetting factor as 0.99.

As shown in Fig. 15, the FRLS-based EKF has the largest amount of computation while having the smallest SOC RMSE. On the contrary, the conventional EKF has the opposite characteristic. Compared to the conventional EKF, the

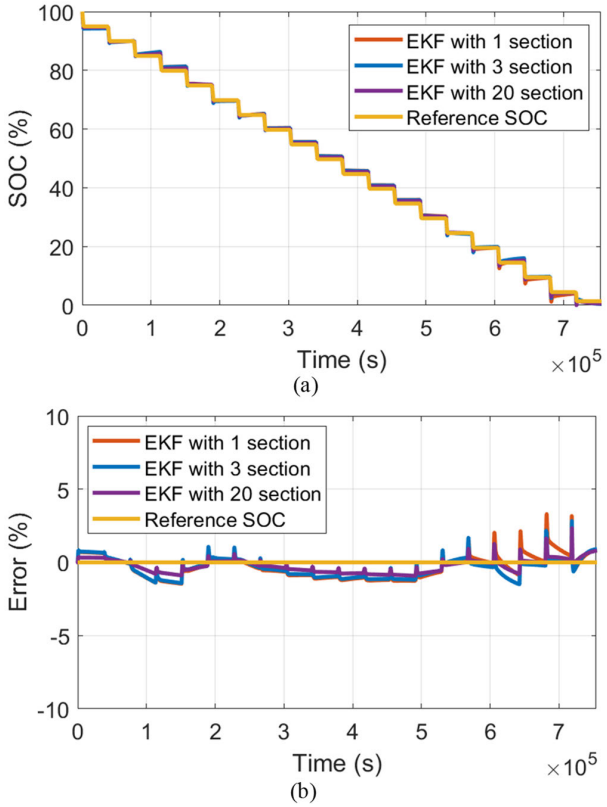


**FIGURE 12.** Simulation result according to section number at 1C-rate (a) SOC estimation at 25 °C (b) SOC estimation error at 25 °C.

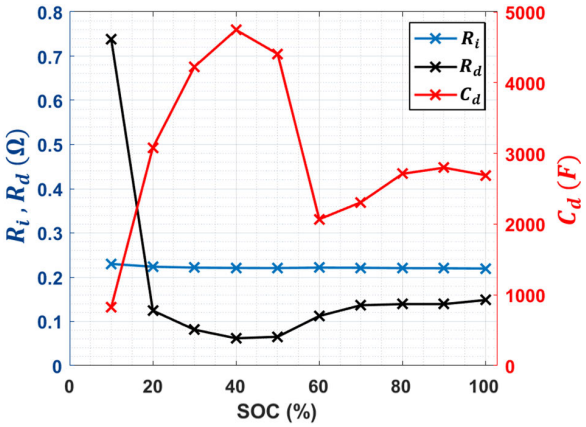


**FIGURE 13.** Battery parameters according to SOC of INR 18650-20R.

**TABLE 6.** Comparison of estimated performance according to section number at 1C-rate 25 °C.

| Section Number | RMSE | Maximum Error (%) | Computation time (s) |
|---|---|---|---|
| 1 | 0.8116 | 3.302 | 2.5336 |
| 3 | 0.752 | 2.8338 | 2.6952 |
| 20 | 0.5094 | 2.3504 | 3.1761 |

proposed EKF has an increased computational time of 10%. However, the relative Percentage Difference (RPD) of RMSE was decreased by 23%, which is greater than the RPD (10%)

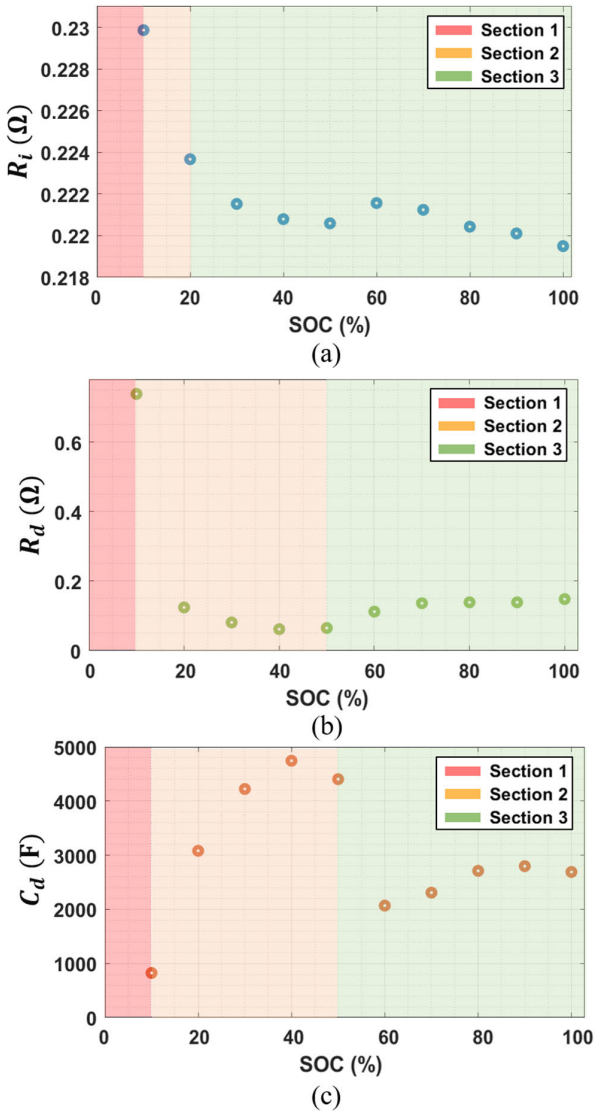


**FIGURE 14.** Battery parameter curve of INR 18650-20R divided into three SOC sections by the proposed method.

**TABLE 7.** Main specifications of INR18650-20R.

| Parameter | Value |
|---|---|
| Nominal capacity | 4900 mAh |
| Charging cutoff voltage | 4.2 V |
| Nominal voltage | 3.7 V |
| Discharging cutoff voltage | 2.5 V |

of computational time. In the comparison of the proposed EKF and FRLS-based EKF, the RPD of RMSE increased by 40%, but the RPD of computational time decreased by 100%. If performance is defined as the difference between RPD of computation time and RPD of SOC RMSE, the proposed method has the best performance among EKFs. In addition, the user can adjust the calculation time and SOC RMSE according to the number ($N$) of SOC sections as

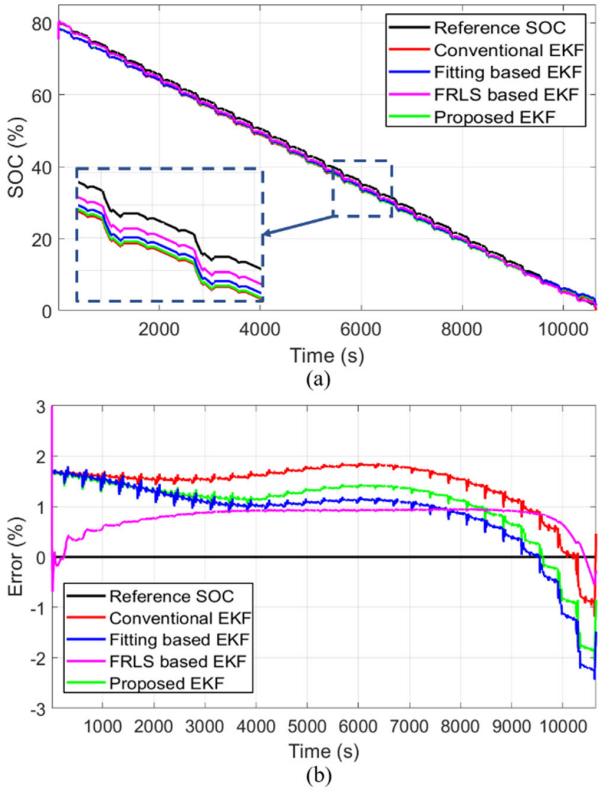


**FIGURE 15.** Comparison of SOC estimation performance of adaptive battery parameter-based EKF and conventional EKF: (a) SOC estimation results, (b) SOC estimation error.

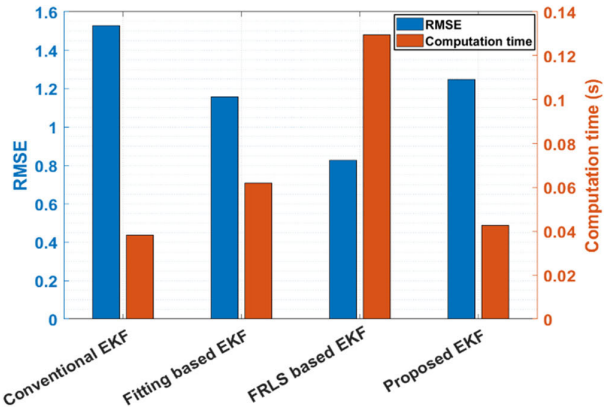


**FIGURE 16.** RMSE and computation time of adaptive battery parameter-based EKF and conventional EKF.

shown in Fig. 6. The proposed method can satisfy the SOC estimation accuracy required by the product with a lower amount of computation than previous EKFs using adaptive battery parameters. For this reason, it is more likely to be applied to commercial products than other improved EKFs.

## VI. CONCLUSION

An enhanced EKF with adaptive battery parameters that change according to the SOC was proposed to improve SOC estimation accuracy. For this purpose, the entire SOC was divided into several sections considering the deviation of the parameter values according to the SOC. Subsequently, the average values for each SOC section were calculated, and the values of the battery parameters were updated with the average values according to the SOC. To verify the performance of the proposed EKF, the parameters of commercial Li-ion batteries (Samsung 21700–50E) were extracted with discharge currents of 1C- and 2C-rates at ambient temperatures of 0, 25, and 45 °C, and MATLAB simulations were performed. The proposed EKF achieved more accurate SOC estimation than the conventional EKF under all the simulation conditions by updating the parameters with the average values of each SOC section according to the SOC. Compared to the conventional EKF, the maximum reduced RMSE and maximum error of the proposed method were 49.37% and 56.41%, respectively. The simulation results verify that the proposed method using adaptive battery parameters can improve the SOC estimation accuracy of the EKF. In future research, we intend to verify the performance of the proposed method using various dynamic battery profiles, such as the actual operation of an electric vehicle.

## REFERENCES

[1] R. J. Brodd, "SECONDARY BATTERIESloverview," *Encyclopedia Electrochem. Power Sources*, vol. 4, pp. 254–261, Dec. 2009, doi: 10.1016/B978-044452745-5.00125-8.
[2] H. Dai, B. Jiang, X. Hu, X. Lin, X. Wei, and M. Pecht, "Advanced battery management strategies for a sustainable energy future: Multilayer design concepts and research trends," *Renew. Sustain. Energy Rev.*, vol. 138, Mar. 2021, Art. no. 110480.
[3] K. W. E. Cheng, B. P. Divakar, H. Wu, K. Ding, and H. F. Ho, "Battery-management system (BMS) and SOC development for electrical vehicles," *IEEE Trans. Veh. Technol.*, vol. 60, no. 1, pp. 76–88, Jan. 2011.
[4] H. Gabbar, A. Othman, and M. Abdussami, "Review of battery management systems (BMS) development and industrial standards," *Technologies*, vol. 9, no. 2, p. 28, Apr. 2021.
[5] Z.-Y. Hou, P.-Y. Lou, and C.-C. Wang, "State of charge, state of health, and state of function monitoring for EV BMS," in *Proc. IEEE Int. Conf. Consum. Electron. (ICCE)*, Jan. 2017, pp. 310–311.
[6] K.-T. Lee, M.-J. Dai, and C.-C. Chuang, "Temperature-compensated model for lithium-ion polymer batteries with extended Kalman filter state-of-charge estimation for an implantable charger," *IEEE Trans. Ind. Electron.*, vol. 65, no. 1, pp. 589–596, Jan. 2018.
[7] W. Zhou, Y. Zheng, Z. Pan, and Q. Lu, "Review on the battery model and SOC estimation method," *Processes*, vol. 9, no. 9, p. 1685, Sep. 2021.
[8] I. B. Espedal, A. Jinasena, O. S. Burheim, and J. J. Lamb, "Current trends for state-of-charge (SoC) estimation in lithium-ion battery electric vehicles," *Energies*, vol. 14, no. 11, p. 3284, Jun. 2021.
[9] S. Guo and L. Ma, "A comparative study of different deep learning algorithms for lithium-ion batteries on state-of-charge estimation," *Energy*, vol. 263, Jan. 2023, Art. no. 125872.
[10] J. Tian, R. Xiong, J. Lu, C. Chen, and W. Shen, "Battery state-of-charge estimation amid dynamic usage with physics-informed deep learning," *Energy Storage Mater.*, vol. 50, pp. 718–729, Sep. 2022.
[11] E. Almaita, S. Alshkoor, E. Abdelsalam, and F. Almomani, "State of charge estimation for a group of lithium-ion batteries using long short-term memory neural network," *J. Energy Storage*, vol. 52, Aug. 2022, Art. no. 104761.
[12] D. Zhang, C. Zhong, P. Xu, and Y. Tian, "Deep learning in the state of charge estimation for Li-ion batteries of electric vehicles: A review," *Machines*, vol. 10, no. 10, p. 912, Oct. 2022.
[13] Y. Li, B. Xiong, D. M. Vilathgamuwa, Z. Wei, C. Xie, and C. Zou, "Constrained ensemble Kalman filter for distributed electrochemical state estimation of lithium-ion batteries," *IEEE Trans. Ind. Informat.*, vol. 17, no. 1, pp. 240–250, Jan. 2021.
[14] Y. Li, Z. Wei, B. Xiong, and D. M. Vilathgamuwa, "Adaptive ensemble-based electrochemical–thermal degradation state estimation of lithium-ion batteries," *IEEE Trans. Ind. Electron.*, vol. 69, no. 7, pp. 6984–6996, Jul. 2022.

[15] H. He, R. Xiong, X. Zhang, F. Sun, and J. Fan, "State-of-charge estimation of the lithium-ion battery using an adaptive extended Kalman filter based on an improved Thevenin model," *IEEE Trans. Veh. Technol.*, vol. 60, no. 4, pp. 1461–1469, May 2011.
[16] M. Lagraoui, S. Doubabi, and A. Rachid, "SOC estimation of lithium-ion battery using Kalman filter and Luenberger observer: A comparative study," in *Proc. Int. Renew. Sustain. Energy Conf. (IRSEC)*, Oct. 2014, pp. 636–641.
[17] R. Xiong, H. He, F. Sun, and K. Zhao, "Evaluation on state of charge estimation of batteries with adaptive extended Kalman filter by experiment approach," *IEEE Trans. Veh. Technol.*, vol. 62, no. 1, pp. 108–117, Jan. 2013.
[18] H. Rahimi-Eichi, F. Baronti, and M.-Y. Chow, "Online adaptive parameter identification and state-of-charge coestimation for lithium-polymer battery cells," *IEEE Trans. Ind. Electron.*, vol. 61, no. 4, pp. 2053–2061, Apr. 2014.
[19] Y. Kang, C. Zhang, K. Yang, and Q. Gao, "Analysis of the temperature change of a single battery based on simulink," *Int. J. Electrochem. Sci.*, vol. 16, no. 10, Oct. 2021, Art. no. 21107.
[20] N. Andrenacci, F. Vellucci, and V. Sglavo, "The battery life estimation of a battery under different stress conditions," *Batteries*, vol. 7, no. 4, p. 88, Dec. 2021.
[21] V. Sangwan, A. Sharma, R. Kumar, and A. K. Rathore, "Estimation of optimal Li-ion battery parameters considering c-rate, SOC and temperature," in *Proc. 7th India Int. Conf. Power Electron. (IICPE)*, Nov. 2016, pp. 1–6.
[22] S. Yang, S. Zhou, Y. Hua, X. Zhou, X. Liu, Y. Pan, H. Ling, and B. Wu, "A parameter adaptive method for state of charge estimation of lithium-ion batteries with an improved extended Kalman filter," *Sci. Rep.*, vol. 11, no. 1, pp. 1–15, Mar. 2021.
[23] Q. Wang, J. Kang, Z. Tan, and M. Luo, "An online method to simultaneously identify the parameters and estimate states for lithium ion batteries," *Electrochim. Acta*, vol. 289, pp. 376–388, Nov. 2018.
[24] M. Hossain, M. E. Haque, and M. T. Arif, "Kalman filtering techniques for the online model parameters and state of charge estimation of the Li-ion batteries: A comparative analysis," *J. Energy Storage*, vol. 51, Jul. 2022, Art. no. 104174.
[25] Z. Cui, W. Hu, G. Zhang, Z. Zhang, and Z. Chen, "An extended Kalman filter based SOC estimation method for Li-ion battery," *Energy Rep.*, vol. 8, pp. 81–87, 2022.
[26] S. Hong, M. Kang, H. Park, J. Kim, and J. Baek, "Real-time state-of-charge estimation using an embedded board for Li-ion batteries," *Electronics*, vol. 11, no. 13, p. 2010, Jun. 2022.
[27] S. Madani, E. Schaltz, and S. K. Kær, "An electrical equivalent circuit model of a lithium titanate oxide battery," *Batteries*, vol. 5, no. 1, p. 31, Mar. 2019.
[28] I. Baccouche, B. Manai, and N. E. B. Amara, "SoC estimation of LFP battery based on EKF observer and a full polynomial parameters-model," in *Proc. IEEE 91st Veh. Technol. Conf. (VTC-Spring)*, May 2020, pp. 1–5.
[29] G. Zhao and Y. Wang, "An online model identification for state of charge estimation of lithium-ion batteries using extended Kalman filter," in *Proc. IEEE 3rd Int. Conf. Renew. Energy Power Eng. (REPE)*, Oct. 2020, pp. 34–38.
[30] *Data Test for INR 18650-20R Cylindrical Cell*. Accessed: Jan. 5, 2017. [Online]. Available: https://calce.umd.edu/battery-data

**JAEJUNG YUN** (Member, IEEE) received the Ph.D. degree in electric engineering from the Pohang University of Science and Technology, Pohang, South Korea, in 2012.

He was a Senior Researcher with the Samsung Advanced Institute of Technology (SAIT), Suwon, South Korea, where he worked on developing power conversion systems for electric vehicles and renewable energy. He is currently an Assistant Professor with the School of Electrical Engineering, Chungbuk National University, Cheongju-si, South Korea. His research interests include battery management systems, the design and control of power conversion systems, and wireless power transfer systems.

**YEONHO CHOI** was born in Cheonan, South Korea, in January 1997. He received the B.S. degree in electrical engineering from Chungbuk National University, Cheongju, South Korea, in 2022, where he is currently pursuing the M.S. degree in electrical engineering. His research interests include battery management systems and state estimation algorithm.

**JAEHYUNG LEE** was born in Youngju, South Korea, in March 1994. He received the B.S. degree in electrical engineering from Daegu University, Gyeongsan, South Korea, in 2021. He is currently pursuing the M.S. degree in electrical engineering with Chungbuk National University. His current research interests include battery management systems and hardware in loop systems.

**SEONGGON CHOI** (Member, IEEE) received the M.S. (Eng.) and Ph.D. degrees from the Korea Advanced Institute of Science and Technology, Daejeon, South Korea, in 1999 and 2004, respectively. He was with LG Information and Communication, from 1992 to 1998. In 2004, he joined Chungbuk National University, Cheongju, South Korea, as a Professor. His current research interests include broadband network architecture and technologies with a particular emphasis on performance and protocol problems. He has been a member of the ITU-T Study Group 13 on the mobility and new generation network (NGN) issues, since 2002.

**CHANGSEOP SHIN** (Member, IEEE) received the M.S. and Ph.D. degrees from Seoul National University, Seoul, South Korea, in 2002 and 2013, respectively. He is currently an Assistant Professor with the School of Electrical Engineering, Chungbuk National University, Cheongju-si, South Korea. His research interests include energy engineering including energy efficiency and emission reduction in agricultural machinery area, design of agricultural implement, and process development of 3D printing metal.